Ultrafast studies of carrier and magnetization dynamics in GaMnAs

J. P. Zahn, A. Gamouras, S. March, X. Liu, J. K. Furdyna, and K. C. Hall

Citation: Journal of Applied Physics **107**, 033908 (2010); doi: 10.1063/1.3275347
View online: http://dx.doi.org/10.1063/1.3275347
View Table of Contents: http://scitation.aip.org/content/aip/journal/jap/107/3?ver=pdfcov
Published by the AIP Publishing

Ultrafast studies of carrier and magnetization dynamics in GaMnAs

J. P. Zahn,[1] A. Gamouras,[1] S. March,[1] X. Liu,[2] J. K. Furdyna,[2] and K. C. Hall[1,a)]
[1]*Department of Physics and Atmospheric Science, Dalhousie University, Halifax, Nova Scotia B3H1Z9, Canada*
[2]*Department of Physics, University of Notre Dame, Notre Dame, Indiana 46556, USA*

(Received 5 November 2009; accepted 17 November 2009; published online 8 February 2010)

We have investigated the carrier and magnetization dynamics in a GaMnAs structure with perpendicular uniaxial anisotropy using time-resolved pump probe techniques. Experiments were performed over two orders of magnitude variation in pump fluence, revealing an ultrafast demagnetization response that saturates at fluence values larger than 1 mJ/cm^2. Dichroic bleaching contributions exhibit no dependence on the circular polarization state of the pump beam, indicating no signature of electron spin dynamics, in contrast to experiments at similar pump pulse fluence in other III-Mn-V semiconductors. We observe no evidence of a transient hole spin depolarization despite the strong demagnetization effects in our experiments, suggesting that more studies are needed to elucidate the influence of hot holes on the nonlinear optical response of diluted magnetic semiconductors. Differential reflectivity experiments indicate an electron trapping time of 1 ps, followed by carrier recombination on a time scale of several nanoseconds. The demagnetization observed is incomplete, reaching only 80% of the equilibrium magnetization at saturation. We attribute this to the optical saturation of the band edge absorption in GaMnAs. © *2010 American Institute of Physics*. [doi:10.1063/1.3275347]

I. INTRODUCTION

Exploitation of the spin degree of freedom may lead to new semiconductor devices with improved performance and/or enhanced functionality.[1,2] Recent device proposals include low-power spin-sensitive field effect transistors,[3–6] Faraday isolators,[7] spin-sensitive all-optical switching devices,[8,9] and spin-based optical sources.[10] The integration of diluted magnetic semiconductors (DMS) is promising due to their unique combination of semiconducting and magnetic properties, which arises from the carrier mediated ferromagnetic order in these materials. Active control of fundamental magnetic properties of interest [e.g., the Curie temperature (T_c) and the coercive field (H_c)] has been achieved by controlling the background hole population using electrical gates[11,12] or continuous wave optical excitation.[13,14] These demonstrations illustrate the versatility of these materials for applications in future spin-based devices. The development of such devices requires a detailed understanding of the origins of ferromagnetic order in DMS materials. Although considerable progress has been made in recent years,[15–24] the exact nature of the underlying ferromagnetic interactions is still not well understood. For example, the relative importance of impurity band and valence band transport is currently under active debate,[20,22,24] and the importance of Mn interstitials in determining the ferromagnetic properties was the focus of several recent works.[23–26]

Ultrafast optical techniques provide a powerful approach to studying the fundamental interactions governing ferromagnetic order in DMS materials.[27–40] Femtosecond optical excitation leads to a rapid modification of the ferromagnetic properties through the introduction of an excess population of holes. Interrogation of the resulting dynamics with femtosecond resolution using techniques such as time-resolved Kerr rotation allows a direct evaluation of the decay times associated with various excitations in the magnetic and carrier systems, and provides detailed information on the strength of interactions among the relevant constituents (localized spins, holes, and lattice vibrations). Kimel *et al.*[27] studied the spectral dependence of the optically induced magnetization associated with a spin-polarized electron distribution in GaMnAs, revealing an electron spin lifetime of 30 ps. A transient hole-mediated enhancement of both magnetization and T_c was recently observed in GaMnAs by Wang *et al.*[34] An ultrafast reorientation of the magnetic easy axis has also been demonstrated by several groups in recent years,[28,29,31,33,35–39] stimulating complex precession dynamics in the magnetic system. These studies have provided key insights into magnetic anisotropy in DMS systems.

The above demonstrations were carried out under conditions of optically excited hole densities several orders of magnitude lower than the background hole population, leading to a relatively weak perturbation of the ferromagnetic order. For applications of DMS materials as optically addressable nonvolatile memory elements in spin-based devices, strong photoinduced changes to the ferromagnetic state are desirable. In GaMnAs samples with a biaxial in-plane anisotropy, Astakhov *et al.*[41] demonstrated a complete, permanent reversal of the hysteresis loop with the exposure of the sample to a single, high fluence ($\sim$150 mJ/cm^2) optical pulse. Together with recent studies of coercivity dynamics in this system,[42] the experiments of Astakhov *et al.* demonstrate the potential for application of DMS materials in ultrafast multivalued magneto-optical memory devices. Wang *et al.*[43] demonstrated ultrafast magnetization quenching in InMnAs, reaching 100% reduction in ferromagnetic order for optical

a)Electronic mail: kimberley.hall@dal.ca.

pulse fluences exceeding ~10 mJ/cm^2. A model of the observed demagnetization process was proposed in which the p-d exchange interaction leads to a net transfer of angular momentum from the Mn to the hole population.[44] Although recent experiments using mid-IR excitation of GaMnAs provide evidence for the role of hot holes in the demagnetization process,[45] the theoretical model significantly underestimated the size of the demagnetization effect.[44] More work is needed to elucidate the optical response of DMS materials in the highly nonequilibrium, strong photoexcitation regime.

In this paper, we present a comprehensive study of the carrier and magnetization dynamics in GaMnAs using femtosecond pump probe spectroscopy. Optically induced demagnetization dynamics were studied over a broad range of temperatures and pump fluences. We observe a strong ultrafast reduction in ferromagnetic order, accompanied by a subpicosecond, near-complete collapse of the hysteresis loop. Contributions to the pump probe results related to magnetization dynamics and dichroic bleaching are separated through comparison of the pump-induced changes in Kerr rotation and ellipticity.[46] These experiments reveal no signature of a dynamic response of the hole spin polarization, in contrast to recent experiments by Wang *et al.*[45] Beyond the first few picoseconds, the nonlinear optical response is dominated by pump-induced changes in ferromagnetic order. Our power-dependent measurements indicate a saturation of the demagnetization signal for a pump pulse fluence exceeding 1 mJ/cm^2 at 80% of the remanent magnetization, in contrast to findings in InMnAs.[43] We attribute the observed incomplete demagnetization to optical saturation of states near the band gap, in line with similar findings in low-temperature grown GaAs.[47] Differential reflectivity experiments reveal fast (1 ps) electron trapping associated with As antisite defects, followed by a much slower carrier recombination on a time scale of several nanoseconds. Our findings provide insight into the ferromagnetic properties of DMS materials in the highly excited, nonequilibrium regime.

II. SAMPLES AND EXPERIMENTAL METHODS

The sample used in this study was grown by low-temperature molecular beam epitaxy, and consists of 270 nm $Ga_{1-x}Mn_xAs$ ($x \sim 0.03$) grown on a 3.5 μm ZnSe buffer layer on a semi-insulating GaAs substrate. A small lattice mismatch between ZnSe and GaMnAs induces tensile strain in the GaMnAs layer, leading to an easy axis of magnetization along the grown direction.[15–17,48] The results of continuous-wave Kerr rotation measurements on this structure are shown in Fig. 1(a). The observation of square hysteresis loops indicates perpendicular uniaxial anisotropy. [The small linear background apparent in Fig. 1(a) is due to Faraday rotation in the cryostat windows.] The Curie temperature for this structure (which was not subjected to post-growth annealing) is 46 K. The background hole concentration estimated from magnetotransport data is ~1 $\times 10^{20}$ cm^{-3}.

The magnetization dynamics were measured using two-color, time-resolved magneto-optical Kerr effect (TR-MOKE) experiments in the polar configuration.[27,30,46] A

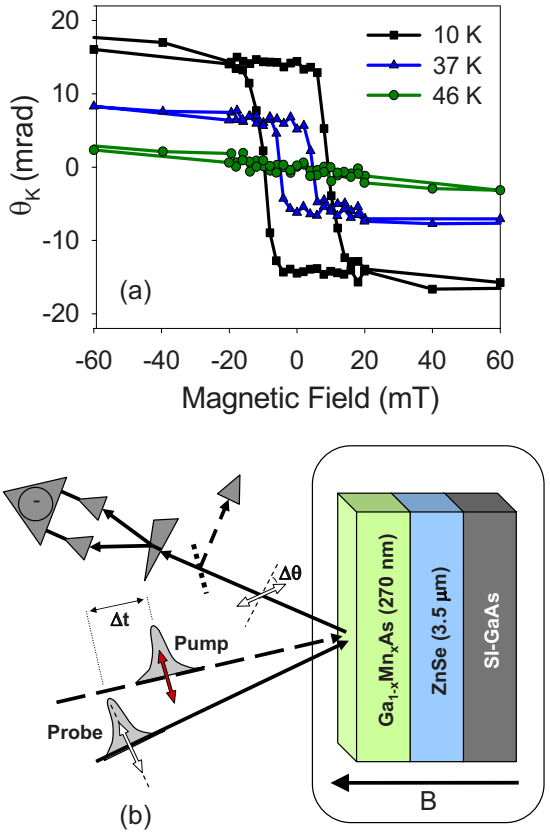

FIG. 1. (Color online) (a) Temperature-dependent Kerr rotation measurements on GaMnAs at a photon energy of 2.03 eV. (b) Schematic of the pump probe experimental setup. The white light probe beam is spectrally resolved using a monochromator (not shown) prior to detection of the TR-MOKE signal (using a Si balanced bridge detector) or the differential reflectivity signal (using a Si photodiode).

schematic of the experimental setup is depicted in Fig. 1(b). The sample was housed in a variable temperature, 7 T, split-coil magneto-optical cryostat. Linearly polarized 800 nm pulses with a duration of 60 fs from a 250 kHz Ti:sapphire laser system were used to excite electron hole pairs in the GaMnAs epilayer. At this pump photon energy, carriers are injected close to the band gap of GaMnAs, minimizing the influence of lattice heating effects due to the optically injected carrier distribution. The pump fluence was in the range 1–10 mJ/cm^2. A tunable white light continuum was generated from a small portion of the 800 nm beam and used as the probe beam. Due to chirp in the white light pulses, the overall time resolution of the setup was ~100 fs. After reflecting from the sample, the probe beam was spectrally resolved using a monochromator, and the Kerr rotation (θ_K) [or the pump-induced change in Kerr rotation ($\Delta\theta_K$)] was measured using a standard polarization bridge and lock-in detection. For TR-MOKE measurements, the Kerr response was detected at a probe photon energy of 2.03 eV. The pump-induced change in the Kerr ellipticity ($\Delta\eta_K$) was also measured under the same conditions through the addition of a quarter waveplate in the reflected probe beam prior to the polarization bridge.[27,46] The signal to noise level in these experiments was limited by the stability of the white light continuum, with a typical noise floor of 1 mrad. For measurements of the carrier trapping and recombination dynam-

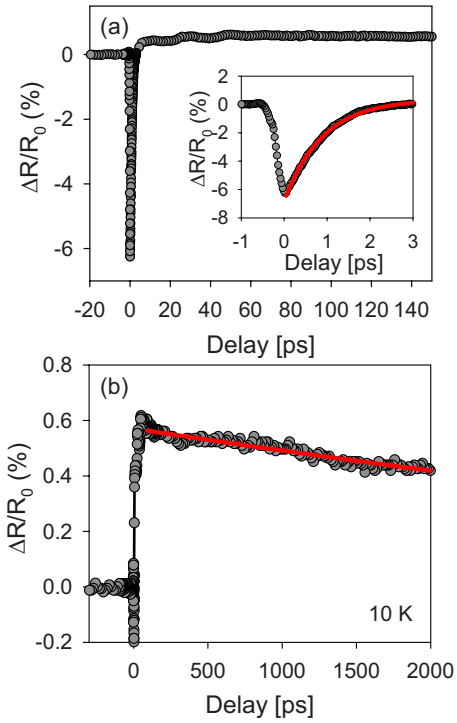

FIG. 2. (Color online) (a) Results of time-resolved differential reflectivity experiments on GaMnAs at 10 K. The inset shows the signal characteristics for a short range of probe pulse delay. The solid curve in the inset shows a single exponential fit, with a time constant of 0.9 ps. (b) Same data as in (a) for the full range of accessible probe pulse delays in the apparatus. The vertical scale was chosen to display the dynamics of the slow positive $\Delta R/R$ signal observed beyond the first few picoseconds. The solid curve indicates a single exponential fit with a time constant of 7 ns. The pump fluence for these data was 7 mJ/cm^2.

ics, differential reflectivity experiments were performed under the same conditions as the TR-MOKE experiments. The pump-induced change in the probe reflectivity, expressed as a percentage of the unsaturated reflectivity, was measured at a probe photon energy of 1.73 eV using a fast silicon photodiode and lock-in detection.

III. RESULTS AND DISCUSSION

A. Carrier dynamics

The results of differential reflectivity experiments on GaMnAs are shown in Fig. 2. The general features observed are similar to those seen previously in InMnAs (Ref. 49) and GaMnAs,[26] as well as in GaAs grown at low substrate temperatures.[50] These features reflect the dominant influence of a large density of As point defects on the carrier dynamics in this material.[25,26,50–52] Immediately following the pump pulse, a large negative $\Delta R/R$ signal is observed. This negative peak is attributed to free carrier (Drude) absorption by the optically injected carrier distribution.[53] Free carrier absorption is enhanced in the presence of a large density of defects due to the partial relaxation of the k-vector conservation rule for optical transitions.[25,26,50,54] Due to the larger effective mass of the holes, the negative $\Delta R/R$ peak in Fig. 2(a) is primarily attributed to free carrier absorption by the optically injected electrons.

The initial negative $\Delta R/R$ signal decays rapidly due to fast electron trapping at As antisite defects.[28,34,55,56] This decay is shown more clearly in the inset to Fig. 2(a). A single exponential fit to these data yields a time constant of 0.9 ps. Similar electron trapping times have been measured in low-temperature-grown GaAs and InP, ranging from a few hundred femtoseconds to 1.6 ps in as-grown samples.[55–57]

For a probe pulse delay larger than a few picoseconds, the differential reflectivity exhibits a much weaker, positive signal. Using a Boltzmann equation formalism, Sanders *et al.*[53] showed that the trapped electron population modifies the complex dielectric response, leading to a positive $\Delta R/R$ signal for photon energies larger than the band gap, in agreement with the results in Fig. 2. A weak oscillation with a period of 20 ps is also observed in the data in Fig. 2(a). Such an oscillation was seen in InMnAs by Wang *et al.*,[49] and was attributed to dynamic Fabry–Perot effects in the buffer layer associated with a coherent acoustic phonon wavepacket. This phonon wavepacket is generated in the DMS layer by the optically injected carrier population through deformation potential coupling.[53] The period of oscillation may be estimated using the probe wavelength, the index of refraction, and the longitudinal acoustic phonon velocity.[30] For the ZnSe buffer layer in the structure investigated here,[58,59] we calculate an oscillation period associated with such a phonon wavepacket to be 30 ps, in reasonable agreement with the measured value.

The positive $\Delta R/R$ signal decays through carrier recombination on a much longer time scale. The full range of accessible probe pulse delay for the experimental apparatus is approximately 2 ns. Using the data over this limited range, we estimate the carrier recombination time to be 7 ns.

B. Ultrafast demagnetization in GaMnAs

The results of TR-MOKE measurements at 10 K are shown in Fig. 3(a) for a short range of probe pulse delay. $\Delta\theta_K$ changes sign with reversal of the external magnetic field and indicates pump-induced demagnetization. A comparison of the shape of the rising edge of the $\Delta\theta_K$ signal for opposite signs of the magnetic field in Fig. 3(a) reveals a magnetic field independent contribution to the nonlinear response during the first picosecond. This contribution is not associated with pump-induced changes in ferromagnetic order, and is discussed in Sec. III C. The TR-MOKE results for a larger range of probe delays are shown in Fig. 3(b). A weak secondary rise is visible in the data after the zero delay peak. This rise increases the $\Delta\theta_K$ signal by ~10% on a time scale of 15 ps. This slower demagnetization process is attributed to spin lattice relaxation,[60–63] in which the excess thermal energy deposited into the lattice by the optically injected carriers leads to heating of the Mn spin system. In earlier demagnetization experiments in InMnAs by Wang *et al.*,[43] spin lattice relaxation was found to have a much stronger influence than in the experiments reported here. This may reflect the larger optical excess energy in these earlier experiments, which leads to enhanced lattice heating by the cooling carrier distribution. (The pump photon energy was ~200 meV

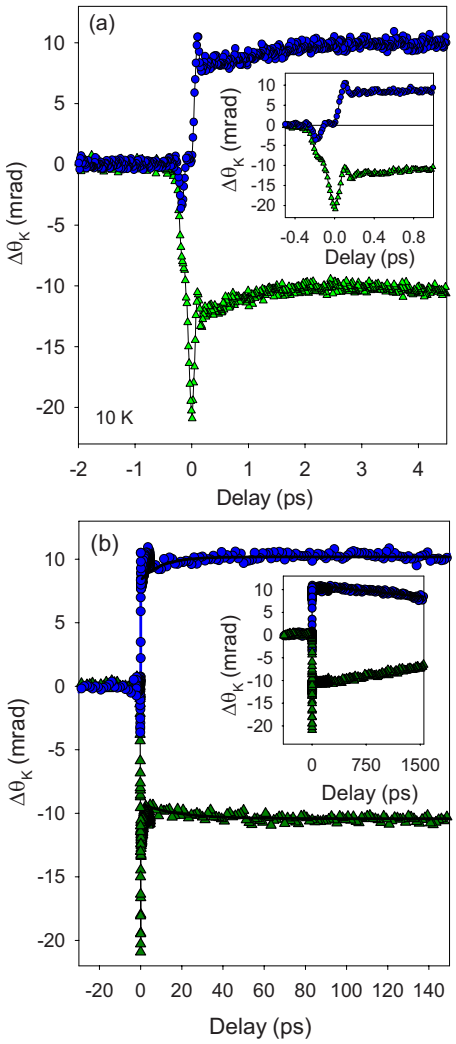

FIG. 3. (Color online) (a) Results of TR-MOKE experiments, showing the pump-induced change in the Kerr rotation ($\Delta\theta_K$) vs probe pulse delay at applied magnetic fields of +180 (circles) and −180 mT (triangles). For these data, the pump beam was linearly polarized, with a fluence of 7 mJ/cm^2. Inset: the same data are shown for a shorter range of probe delay. (b) TR-MOKE results for the same conditions as in (a), showing a larger range of probe pulse delays. A weak (~10%) increase in the magnitude of the $\Delta\theta_K$ signal is apparent in the data on this time scale. Single exponential fits (solid curves) indicate a rise time of ~15 ps.

above the band gap of InMnAs in the work of Wang *et al.*; in the experiments reported here, carriers are injected within 50 meV of the band gap.)

The TR-MOKE signal decays on a much longer time scale, as shown in the inset to Fig. 3(b), indicating recovery of the macroscopic magnetization. Within the limited range of accessible probe pulse delays, the time scale for this recovery process is estimated to be 5 ns. Aside from the first few picoseconds, these signal features are not sensitive to the polarization state of the pump beam, as shown in Fig. 4. The symmetry of the $\Delta\theta_K$ signal for opposite magnetic field directions indicates that, beyond the first few picoseconds, the nonlinear Kerr response is strongly dominated by pump-induced changes in ferromagnetic order.

The pump pulse induces a near-complete collapse of the hysteresis loop, as shown in Fig. 5. The loop appears to be nearly paramagnetic for a probe pulse delay of only 100 fs,

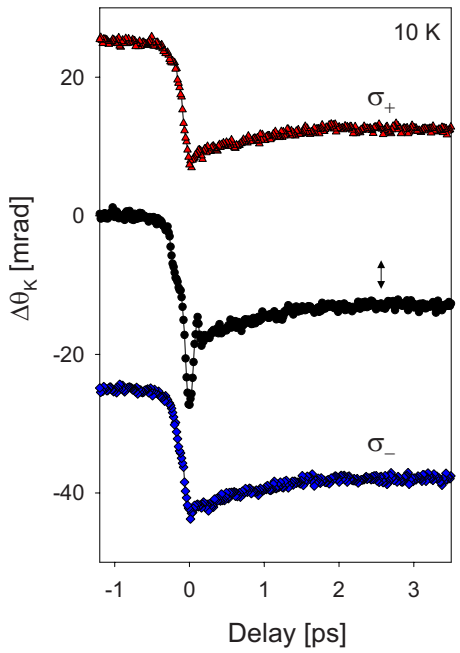

FIG. 4. (Color online) TR-MOKE results for different polarization states of the pump beam (triangles: σ_+; circles: linear; diamonds: σ_-). For all experiments, the probe beam is linearly polarized at 45° to the s and p directions.

indicating an ultrafast magnetic response that exceeds the time resolution of these experiments. The hysteresis loop for positive probe pulse delay is similar to observations in $CoPt_3$ alloy films, in which a full collapse of the hysteresis loop was observed within 120 fs.[64]

A model for the ultrafast demagnetization process was proposed by Cywiński *et al.*[44] Prior to the pump pulse, the system is in an equilibrium state in which both Mn and hole spins are polarized (well below T_C). The pump pulse injects a large density of excess holes with a random spin polarization, bringing the hole-Mn system far from equilibrium. These excess holes stimulate a rapid transfer of spin angular momentum from the Mn spin system to the holes. The hole spin relaxation time is expected to be very short in DMS systems (<100 fs) due to strong spin-orbit mixing in the valence bands[65] and the large density of defects, which leads

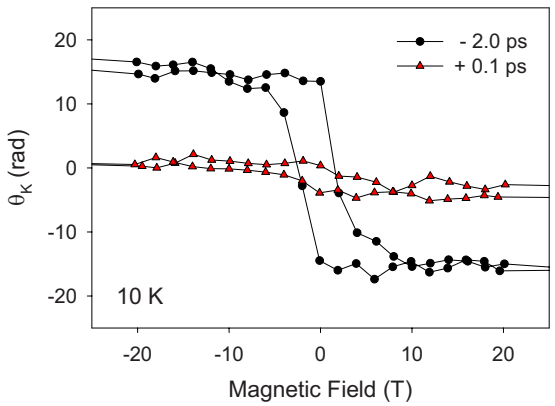

FIG. 5. (Color online) MOKE measurements of the magnetic hysteresis loop for probe time delays of −2 ps (circles) and +100 fs (triangles). The pump beam polarization and fluence are the same as those in Fig. 3.

to fast momentum (and spin) relaxation.[66] The angular momentum transferred to the hole system is therefore rapidly dissipated to the lattice.

As indicated in Fig. 4, no difference is observed in the TR-MOKE response for left and right circular polarizations of the pump pulse. This indicates the absence of any detectable spin polarization signal associated with the optically injected carrier population. A Kerr response due to optically injected spin-polarized electrons has been observed in earlier experiments on GaMnAs by Kimel *et al.*,[27] although the pump fluence was several orders of magnitude lower than in the experiments reported here. The lack of polarization dependence we observe is consistent with recent studies of demagnetization dynamics in GaMnAs by Wang *et al.*[45] In that work, the pump pulse fluence was similar to that used in the experiments reported here; however, the pump photon energy was tuned well below the GaMnAs band gap (0.62 eV). This low pump photon energy leads to the excitation of valence states only. The absence of a polarization dependence was therefore attributed by Wang *et al.* to the short hole spin relaxation time. The absence of an electron spin polarization signal in the experiments reported here (despite the optical excitation of both electrons and holes) is not understood. Our observations are also in contrast to recent experiments in InMnAs (Ref. 67) and InMnSb,[68] in which electron spin relaxation dynamics were detected for pump fluences similar to those used here. More work is needed to understand the influence of defect distributions and carrier density variations on the electron and hole spin relaxation dynamics in DMS systems.

C. Dichroic bleaching

The polar Kerr rotation (θ_K) and Kerr ellipticity (η_K) are proportional to the growth direction component of the magnetization (M_z),

$$\theta_K = fM_z \quad \text{and} \quad \eta_K = gM_z, \tag{1}$$

where the coefficients f and g depend on the index of refraction and absorption coefficients for left and right circularly polarized light.[69] The nonlinear Kerr rotation is

$$\Delta\theta_K = f\Delta M_z + \Delta f M_z, \tag{2}$$

with a similar expression for $\Delta\eta_K$. The first term in Eq. (2) indicates the pump-induced change in the magnetization, while the second term represents a purely optical contribution to the nonlinear response, often referred to as *dichroic bleaching*.[46] It is clear from Eq. (2) that a comparison of the dynamic response of $\Delta\theta_K$ and $\Delta\eta_K$ allows the dichroic bleaching contribution to be isolated. The results of this comparison are shown in Figs. 6(a) and 6(b). The difference in the delay dependence of the $\Delta\theta_K$ and $\Delta\eta_K$ signals persists for the first few picoseconds, as shown in the inset to Fig. 6(a). The dichroic bleaching signal exhibits a strong peak at zero delay, followed by a slower component that decays on a time scale of 1.1 ps. The same features are also apparent from averaging the $\Delta\theta_K$ signals for +180 and −180 mT, as shown in Figs. 6(c) and 6(d). These dichroic bleaching contributions were found to be independent of temperature (within 10%)

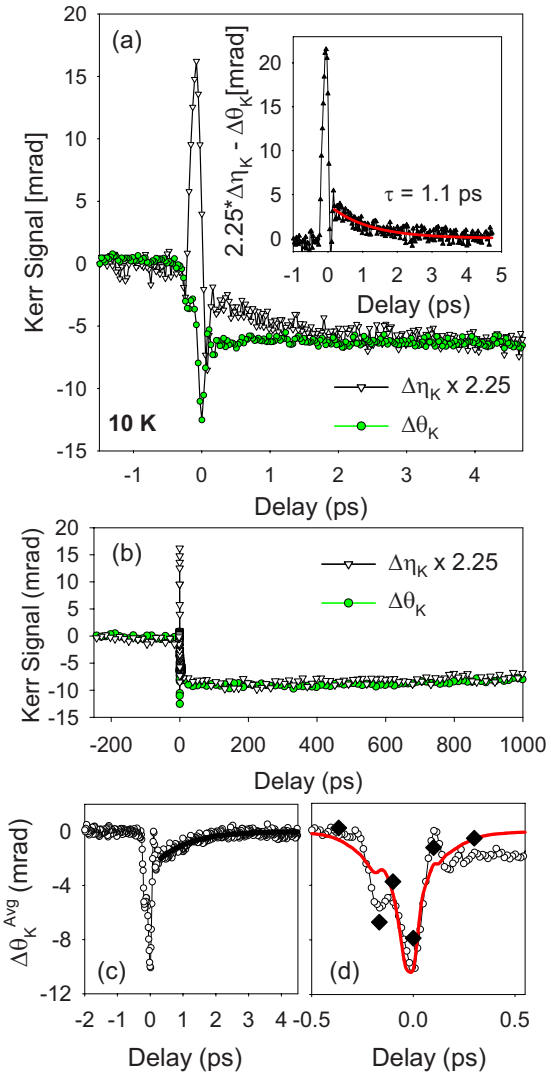

FIG. 6. (Color online) Comparison of the pump-induced change in the Kerr rotation (circles) and Kerr ellipticity (triangles) at an applied magnetic field of −54 mT, showing the importance of dichroic bleaching contributions. The pump beam polarization and fluence are the same as those in Fig. 3. The $\Delta\eta_K$ curve has been scaled by a factor of 2.25 in order to match the signal strengths for long delays. The difference between the two data sets is shown in the inset, together with a single exponential fit to the slow component (solid curve) with a time constant of 1.1 ps. (b) Same data as in (a) shown for a larger range of probe pulse delays. (c) The average of the $\Delta\theta_K$ signals for positive and negative applied magnetic fields. A single exponential fit to the slower signal component is also shown (solid curve), with a time constant of 1 ps. (d) Same data as (c) on a shorter time scale, plotted with the cross correlation of the pump and probe beams (solid curve) and the measured shift of the hysteresis loop vs time delay (diamonds).

between 10 and 50 K, further confirming that they are not tied to the demagnetization dynamics induced by the pump pulse. The delay dependences of $\Delta\theta_K$ and $\Delta\eta_K$ are identical on longer time scales, as shown in Fig. 6(b), indicating that the demagnetization dynamics dominate the optical response beyond the first few picoseconds.

As discussed in Sec. III B, the TR-MOKE response is identical for left and right circularly polarized pump excitations (Fig. 4) and consequently the dichroic bleaching signal we observe cannot be caused by a net spin polarization in the optically injected carrier distribution. Through measurement of the hysteresis loop for a variety of time delays in the range

of pulse overlap, it was determined that the strong peak at zero delay in the dichroic bleaching signal corresponds to a transient downward shift of the hysteresis loop. The measured loop shift is shown in Fig. 6(d) (diamonds). The results in Fig. 4 indicate that the zero delay peak is strongest for linearly polarized excitation. This suggests that the zero delay peak is caused by a four-wave mixing contribution to the pump probe signal, often referred to as a coherent artifact.[32,70–72] Four-wave mixing signal contributions related to excitation-induced dephasing lead to a transient peak that is strongest for linearly polarized pump and probe beams.[70–72] The time scale for decay of the slower relaxation component in the dichroic bleaching signal is consistent with the electron trapping time measured in the differential reflectivity results. As a result, this slower signal is likely tied to the optically injected electrons, although the exact nature of the nonlinearity [free carrier absorption, (spin-independent) state filling, etc.] is not clear.

In demagnetization studies in GaMnAs by Wang *et al.*,[45] the TR-MOKE signal exhibited a prominent overshoot during the first few picoseconds that was identified as a dichroic bleaching contribution. An interpretation of this feature was proposed in terms of a transient depolarization of the hole spins through spin flip scattering with the Mn spins during demagnetization. This interpretation was supported by the observation that the overshoot feature reversed in sign with reversal of the external magnetic field, indicating that it was tied to the magnetization dynamics. In their experiments, Wang *et al.* used a probe photon energy close to the optical band gap (1.6 eV). This was thought to enhance the optical nonlinearity associated with state filling in the valence band relative to previous experiments in InMnAs, in which no such hole-related signal was observed.[43] Since the dichroic bleaching signal contributions in Fig. 6(a) are insensitive to changes in the temperature or the external magnetic field, they are not related to a dynamic hole spin polarization. The magnitude of the demagnetization response we observe is comparable to the experiments of Wang *et al.*;[45] yet no evidence of a nonequilibrium hole polarization response was observed for the full range of probe photon energies used (1.77–2.12 eV). This suggests that such a response must be spectrally isolated very close to the band edge. More studies of the spectral dependence of the nonlinear Kerr response of DMS semiconductors are needed to clarify the role of nonequilibrium hole spin dynamics.

D. Temperature dependence

The TR-MOKE signal is shown for a range of temperatures and magnetic fields in Fig. 7(a). $\Delta\theta_K$ decreases strongly with increasing temperature. In the data taken at 50 K, only the dichroic bleaching contribution remains. The magnitude of the $\Delta\theta_K$ signal at a fixed time delay of 100 ps is shown versus sample temperature in Fig. 7(b), along with the linear Kerr rotation. $\Delta\theta_K$ vanishes for $T > T_C$. Together with the similar delay dependence of $\Delta\theta_K$ and $\Delta\eta_K$ in Fig. 6(b), the temperature dependence in Fig. 7 provides further indication that the demagnetization effect is the only source of the optical Kerr nonlinearity beyond the first few picoseconds.

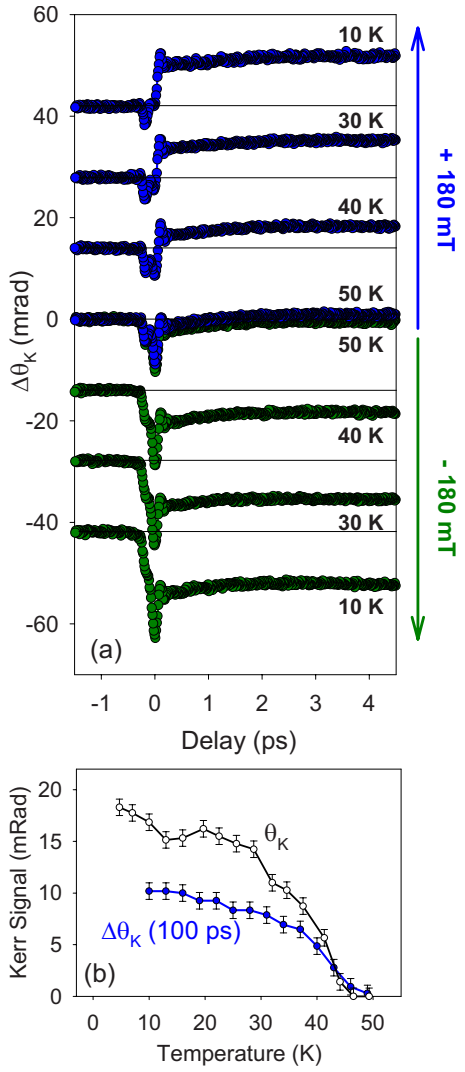

FIG. 7. (Color online) (a) Delay-dependent TR-MOKE results for a range of sample temperatures, indicating a rapid decrease in $\Delta\theta_K$ with increasing temperature. The pump beam polarization and fluence are the same as those in Fig. 3. (b) The magnitude of the $\Delta\theta_K$ signal at a probe pulse delay of 100 ps is shown vs sample temperature, together with the linear MOKE response.

No evidence for enhancement in the Curie temperature may be seen in the data in Fig. 7, in contrast to the findings of Wang *et al.*[34] Demagnetization effects dominate the optical response in the experiments reported here due to the much larger pump fluence used. It should also be noted that the enhancement effects observed in Ref. 34 required a large applied magnetic field (1 T) due to the in-plane easy axis for the GaMnAs structure studied in that work. It is not clear if any enhancement effects would be observed in our experiments for comparable pump fluences to those used in Ref. 34, as a much smaller external magnetic field (~10 mT) is required to saturate the magnetization along the growth direction. Experiments examining the complex interplay between demagnetization effects and a possible photoinduced paramagnetic to ferromagnetic phase transition in tensile strained DMS systems would be of interest.

E. Power dependence

TR-MOKE experiments were performed over a range of pump fluence spanning two orders of magnitude. The results

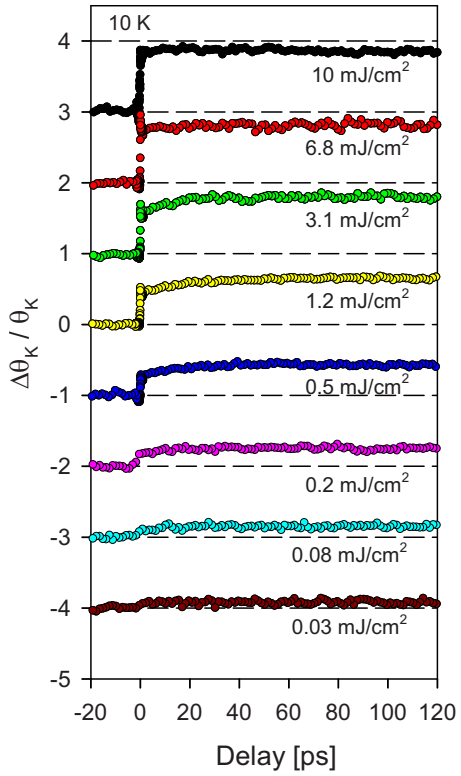

FIG. 8. (Color online) (a) TR-MOKE results for a range of pump pulse fluences. These data were taken at an applied magnetic field of 54 mT. The data for different pump fluence values are offset for clarity.

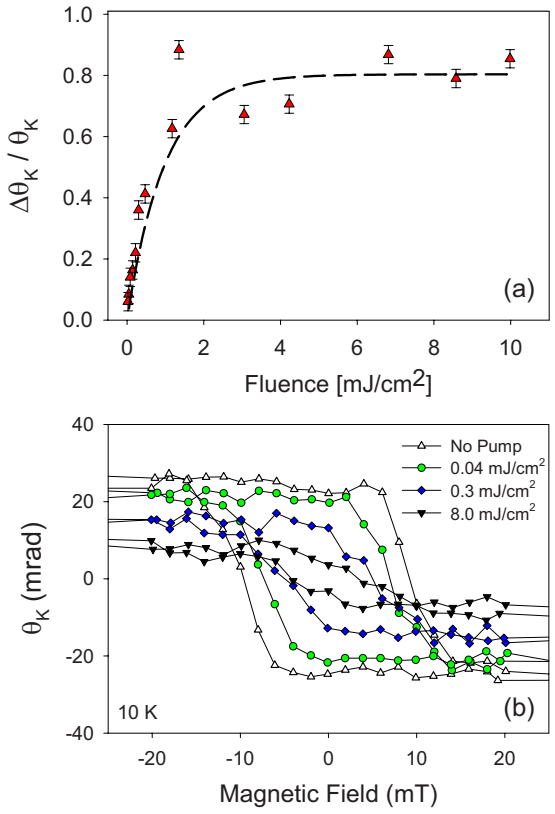

FIG. 9. (Color online) (a) The magnitude of $\Delta\theta_K/\theta_K$ at a fixed time delay of 150 ps is plotted vs pump pulse fluence. A fit of the data to a saturation function is also shown (dashed curve). (b) The Kerr rotation vs external magnetic field for different values of pump pulse fluence. The hysteresis loop with no pump beam on the sample is also shown for comparison.

of these experiments are shown in Figs. 8 and 9. The vertical axis in Fig. 8 shows the ratio $\Delta\theta_K/\theta_K$, highlighting the absolute magnitude of the demagnetization response. The secondary rise is reduced below the signal to noise level for a pump fluence exceeding ~ 3 mJ/cm^2. This suggests that direct hole-Mn spin coupling dominates the demagnetization process for these high fluence values, with a progressively weaker role played by spin lattice relaxation as the pump fluence is increased. These findings are similar to earlier reports of demagnetization dynamics in InMnAs.[43] The magnitude of $\Delta\theta_K/\theta_K$ for a fixed probe pulse delay of 150 ps is plotted versus pump fluence in Fig. 9(a). The demagnetization effect is observed to saturate for a pump fluence greater than ~ 1 mJ/cm^2. A similar saturation was observed in InMnAs,[43] although with a saturated value of $\Delta\theta_K/\theta_K$ of unity. In contrast, in our experiments, the saturated value is only ~ 0.8. The linear Kerr response is shown in Fig. 9(b) for different values of the pump fluence. These hysteresis loops were measured at a probe pulse delay of 4 ps. A weak hysteresis is apparent in the data in Fig. 9(b) for the largest pump fluence. Together with the observation of a maximum $\Delta\theta_K/\theta_K$ less than unity, this indicates that the demagnetization process is incomplete.

We attribute the saturation of $\Delta\theta_K/\theta_K$ in Fig. 9(a) to the saturation of the absorption coefficient in GaMnAs. In the demagnetization experiments in InMnAs, the pump photon energy exceeded the optical band gap energy by 200 meV.[43] In the experiments we report here, the photon energy of the pump beam (1.55 eV) was close to the GaMnAs band gap energy,[73] where the density of states is much lower. Power-dependent absorption measurements were done for a range of wavelengths and pulse durations in low-temperature-grown GaAs by Loka *et al.*[47,56] Strong saturation effects were observed in those experiments, despite band tailing associated with the large density of As antisite defects introduced during low-temperature growth.[20] For excitation conditions similar to those used here, the optical absorption was observed by Loka *et al.* to saturate at a pump fluence of 1.5 mJ/cm^2. This is in good agreement with the results in Fig. 9(a). Saturation of the optical transition implies that the hole density generated by the pump pulse is constant for a pump fluence above 1 mJ/cm^2, leading to a saturation in the magnitude of the demagnetization response.

The absorption coefficient in GaMnAs increases sharply with increasing photon energy.[20] We would therefore expect stronger demagnetization effects for shorter pump wavelengths. It may also be possible to increase the magnitude of the demagnetization effect by varying the optical pulse duration, since a reduced pulse duration would increase the relative importance of multiphoton absorption processes.[47,56]

IV. CONCLUSIONS

In summary, the carrier and magnetization dynamics have been studied in GaMnAs using femtosecond pump probe spectroscopy. The TR-MOKE response changes sign with reversal of the external magnetic field direction, and disappears above T_C, indicating femtosecond optical control

of ferromagnetic order. The sign of the $\Delta\theta_K$ signal and the shape of the hysteresis loop indicate a rapid demagnetization effect that turns on in less than 100 fs. The carrier dynamics in this structure were studied using time-resolved differential reflectivity experiments. These measurements indicate an electron trapping time of 1 ps due to As antisite defects, consistent with previous studies in InMnAs (Ref. 49) and low-temperature grown III-V semiconductors.[55–57] Carrier recombination was observed on a much longer time scale of several nanoseconds.

Measurements for different circular polarization states of the pump beam indicate no electron spin polarization response, in contrast to earlier experiments on GaMnAs at a much lower pump fluence by Kimel *et al.*[27] In recent high fluence experiments in GaMnAs by Wang *et al.* the absence of a polarization dependence in TR-MOKE experiments was attributed to the midinfrared excitation wavelength, which leads to excitation of valence states only;[45] however, the experiments we report here suggest that this observation is more general. These findings indicate the need for more studies of electron spin kinetics in DMSs. Dichroic bleaching signal contributions identified through a comparison of the Kerr rotation and ellipticity dynamics were found to be insensitive to changes in external magnetic field or temperature, indicating no TR-MOKE signal contribution associated with a dynamic hole depolarization. This suggests that the transient hole spin signal observed in recent experiments by Wang *et al.*[45] may only manifest for a probe wavelength near the peak of the magneto-optical response of GaMnAs.

TR-MOKE experiments over more than two orders of magnitude variation in pump fluence reveal a saturation in the magnetic response for a pump fluence exceeding 1 mJ/cm^2. The maximum change in the Kerr rotation is 80% of the equilibrium Kerr signal, and the linear Kerr response maintains a finite coercivity at all fluence values, indicating an incomplete demagnetization of the sample. This saturation is attributed to the low density of states at 1.55 eV in GaMnAs, which leads to saturation of the optical absorption despite defect-induced band tailing. Our findings provide insight into the highly nonequilibrium carrier and magnetization dynamics in DMS materials in the strong excitation regime.

ACKNOWLEDGMENTS

This research is supported by the Canada Foundation for Innovation, the Natural Sciences and Engineering Research Council of Canada, the Canada Research Chairs Program, the National Science Foundation (Grant No. DMR-0603752), and the Lockheed Martin Corporation.

[1]S. A. Wolf, D. D. Awschalom, R. A. Buhrman, J. M. Daughton, S. von Molnar, M. L. Roukes, A. Y. Chtchelkanova, and D. M. Treger, Science **294**, 1488 (2001).
[2]*Semiconductor Spintronics and Quantum Computation*, edited by D. D. Awschalom, D. Loss, and N. Samarth (Springer-Verlag, Berlin, 2002).
[3]S. Datta and B. Das, Appl. Phys. Lett. **56**, 665 (1990).
[4]K. C. Hall, W. H. Lau, K. Gündoğdu, M. E. Flatté, and T. F. Boggess, Appl. Phys. Lett. **83**, 2937 (2003).
[5]K. C. Hall and M. E. Flatté, Appl. Phys. Lett. **88**, 162503 (2006).
[6]J. Schliemann, J. Carlos Egues, and D. Loss, Phys. Rev. Lett. **90**, 146801 (2003).
[7]K. Onodera, T. Masumoto, and M. Kimura, Electron. Lett. **30**, 1954 (1994).
[8]Y. Nishikawa, A. Tackeuchi, S. Nakamura, S. Muto, and N. Yokoyama, Appl. Phys. Lett. **66**, 839 (1995).
[9]K. C. Hall, S. W. Leonard, H. M. van Driel, A. R. Kost, E. Selvig, and D. H. Chow, Appl. Phys. Lett. **75**, 4156 (1999).
[10]J. Rudolph, D. Hägele, H. M. Gibbs, G. Khitrova, and M. Oestreich, Appl. Phys. Lett. **82**, 4516 (2003).
[11]H. Ohno, D. Chiba, F. Matsukura, T. Omiya, E. Abe, T. Dietl, Y. Ohno, and K. Ohtani, Nature (London) **408**, 944 (2000).
[12]D. Chiba, M. Yamanouchi, F. Matsukura, and H. Ohno, Science **301**, 943 (2003).
[13]S. Koshihara, A. Oiwa, M. Hirasawa, S. Katsumoto, Y. Iye, C. Urano, H. Takagi, and H. Munekata, Phys. Rev. Lett. **78**, 4617 (1997).
[14]A. Oiwa, T. Slupinski, and H. Munekata, Appl. Phys. Lett. **78**, 518 (2001).
[15]T. Dietl, H. Ohno, F. Matsukura, J. Cibert, and D. Ferrand, Science **287**, 1019 (2000).
[16]T. Dietl, H. Ohno, and F. Matsukura, Phys. Rev. B **63**, 195205 (2001).
[17]M. Abolfath, T. Jungwirth, J. Brum, and A. H. MacDonald, Phys. Rev. B **63**, 054418 (2001).
[18]J. König, T. Jungwirth, and A. H. MacDonald, Phys. Rev. B **64**, 184423 (2001).
[19]D. J. Priour, E. H. Hwang, and S. Das Sarma, Phys. Rev. Lett. **92**, 117201 (2004).
[20]K. S. Burch, J. Stephens, R. K. Kawakami, D. D. Awschalom, and D. N. Basov, Phys. Rev. B **70**, 205208 (2004).
[21]L. V. Titova, M. Kutrowski, X. Liu, R. Chakarvorty, W. L. Lim, T. Wojtowicz, J. K. Furdyna, and M. Dobrowolska, Phys. Rev. B **72**, 165205 (2005).
[22]L. P. Rokhinson, Y. Lyanda-Geller, Z. Ge, S. Shen, X. Liu, M. Dobrowolska, and J. K. Furdyna, Phys. Rev. B **76**, 161201(R) (2007).
[23]Y. Takeda, M. Kobayashi, T. Okane, T. Ohkochi, J. Okamoto, Y. Saitoh, K. Kobayashi, H. Yamagami, A. Fujimori, A. Tanaka, J. Okabayashi, M. Oshima, S. Ohya, P. N. Hai, and M. Tanaka, Phys. Rev. Lett. **100**, 247202 (2008).
[24]V. G. Storchak, D. G. Eshchenko, E. Morenzoni, T. Prokscha, A. Suter, X. Liu, and J. K. Furdyna, Phys. Rev. Lett. **101**, 027202 (2008).
[25]K. J. Yee, D. Lee, X. Liu, W. L. Lim, M. Dobrowolska, J. K. Furdyna, Y. S. Lim, K. G. Lee, Y. H. Ahn, and D. S. Kim, J. Appl. Phys. **98**, 113509 (2005).
[26]S. Kim, E. Oh, J. U. Lee, D. S. Kim, S. Lee, and J. K. Furdyna, Appl. Phys. Lett. **88**, 262101 (2006).
[27]A. V. Kimel, G. V. Astakhov, G. M. Schott, A. Kirilyuk, D. R. Yakovlev, G. Karczewski, W. Ossau, G. Schmidt, L. W. Molenkamp, and Th. Rasing, Phys. Rev. Lett. **92**, 237203 (2004).
[28]Y. Mitsumori, A. Oiwa, T. Slupinski, H. Maruki, Y. Kashimura, F. Minami, and H. Munekata, Phys. Rev. B **69**, 033203 (2004).
[29]A. Oiwa, H. Takechi, and H. Munekata, J. Supercond. **18**, 9 (2005).
[30]J. Wang, C. Sun, Y. Hashimoto, J. Kono, G. A. Khodaparast, L. Cywiński, L. J. Sham, G. D. Sanders, C. J. Stanton, and H. Munekata, J. Phys.: Condens. Matter **18**, R501 (2006).
[31]D. M. Wang, Y. H. Ren, X. Liu, J. K. Furdyna, M. Grimsditch, and R. Merlin, Phys. Rev. B **75**, 233308 (2007).
[32]K.-J. Han, J.-H. Kim, K.-J. Yee, X. Liu, J. K. Furdyna, and F. Hache, J. Appl. Phys. **101**, 063519 (2007).
[33]J. Qi, Y. Xu, N. H. Tolk, X. Liu, J. K. Furdyna, and I. E. Perakis, Appl. Phys. Lett. **91**, 112506 (2007).
[34]J. Wang, I. Cotoros, K. M. Dani, X. Liu, J. K. Furdyna, and D. S. Chemla, Phys. Rev. Lett. **98**, 217401 (2007).
[35]Y. Hashimoto, S. Kobayashi, and H. Munekata, Phys. Rev. Lett. **100**, 067202 (2008).
[36]E. Rozkotová, P. Němec, P. Horodyská, D. Sprinzl, F. Trojánek, P. Malý, V. Novák, K. Olejník, M. Cukr, and T. Jungwirth, Appl. Phys. Lett. **92**, 122507 (2008).
[37]E. Rozkotová, P. Němec, N. Tesařová, P. Malý, V. Novák, K. Olejník, M. Cukr, and T. Jungwirth, Appl. Phys. Lett. **93**, 232505 (2008).
[38]J. Wang, I. Cotoros, D. S. Chemla, X. Liu, J. K. Furdyna, J. Chovan, and I. E. Perakis, Appl. Phys. Lett. **94**, 021101 (2009).
[39]Y. Hashimoto and H. Munekata, Appl. Phys. Lett. **93**, 202506 (2008).
[40]K. S. Burch, D. D. Awschalom, and D. N. Basov, J. Magn. Magn. Mater. **320**, 3207 (2008).
[41]G. V. Astakhov, A. V. Kimel, G. M. Schott, A. A. Tsvetkov, A. Kirilyuk, D. R. Yakovlev, G. Karczewski, W. Ossau, G. Schmidt, L. W. Molenkamp, and Th. Rasing, Appl. Phys. Lett. **86**, 152506 (2005).

[42]K. C. Hall, J. P. Zahn, A. Gamouras, S. March, J. L. Robb, X. Liu, and J. K. Furdyna, Appl. Phys. Lett. **93**, 032504 (2008).
[43]J. Wang, C. Sun, J. Kono, A. Oiwa, H. Munekata, L. Cywiński, and L. J. Sham, Phys. Rev. Lett. **95**, 167401 (2005).
[44]L. Cywiński and L. J. Sham, Phys. Rev. B **76**, 045205 (2007).
[45]J. Wang, L. Cywiński, C. Sun, J. Kono, H. Munekata, and L. J. Sham, Phys. Rev. B **77**, 235308 (2008).
[46]B. Koopmans, M. van Kampen, J. T. Kohlhepp, and W. J. M. de Jonge, Phys. Rev. Lett. **85**, 844 (2000).
[47]H. S. Loka, S. D. Benjamin, and P. W. E. Smith, Opt. Commun. **155**, 206 (1998).
[48]X. Liu, Y. Sasaki, and J. K. Furdyna, Phys. Rev. B **67**, 205204 (2003).
[49]J. Wang, Y. Hashimoto, J. Kono, A. Oiwa, H. Munekata, G. D. Sanders, and C. J. Stanton, Phys. Rev. B **72**, 153311 (2005).
[50]S. Gupta, M. Y. Frankel, J. A. Valdmanis, J. F. Whitaker, G. A. Mourou, F. W. Smith, and A. R. Calawa, Appl. Phys. Lett. **59**, 3276 (1991).
[51]S. Janz, U. G. Akano, and I. V. Mitchell, Appl. Phys. Lett. **68**, 3287 (1996).
[52]F. Ganikhanov, G.-R. Lin, W.-C. Chen, C.-S. Chang, and C.-L. Pan, Appl. Phys. Lett. **67**, 3465 (1995).
[53]G. D. Sanders, C. J. Stanton, J. Wang, J. Kono, A. Oiwa, and H. Munekata, Phys. Rev. B **72**, 245302 (2005).
[54]J. Kuhl, E. O. Göbel, Th. Pfeiffer, and A. Jonietz, Appl. Phys. A: Mater. Sci. Process. **34**, 105 (1984).
[55]A. J. Lochtefeld, M. R. Melloch, J. C. P. Chang, and E. S. Harmon, Appl. Phys. Lett. **69**, 1465 (1996).
[56]H. S. Loka, S. D. Benjamin, and P. W. E. Smith, IEEE J. Quantum Electron. **34**, 1426 (1998).
[57]Y. Kostoulas, L. J. Waxer, I. A. Walmsley, G. W. Wicks, and P. M. Fauchet, Appl. Phys. Lett. **66**, 1821 (1995).
[58]J. Sörgel and U. Scherz, Eur. Phys. J. B **5**, 45 (1998).
[59]D. T. F. Marple, J. Appl. Phys. **35**, 539 (1964).
[60]T. Strutz, A. M. Witowski, and P. Wyder, Phys. Rev. Lett. **68**, 3912 (1992).
[61]X. Wang, M. Dahl, D. Heiman, P. A. Wolff, and P. Becla, Phys. Rev. B **46**, 11216 (1992).
[62]W. Farah, D. Scalbert, and M. Nawrocki, Phys. Rev. B **53**, R10461 (1996).
[63]M. K. Kneip, D. R. Yakovlev, M. Bayer, A. A. Maksimov, I. I. Tartakovskii, D. Keller, W. Ossau, L. W. Molenkamp, and A. Waag, Phys. Rev. B **73**, 035306 (2006).
[64]E. Beaurepaire, M. Maret, V. Halté, J.-C. Merle, A. Daunois, and J.-Y. Bigot, Phys. Rev. B **58**, 12134 (1998).
[65]M. Krauß, M. Aeschlimann, and H. C. Schneider, Phys. Rev. Lett. **100**, 256601 (2008).
[66]T. Jungwirth, M. Abolfath, J. Sinova, J. Kučera, and A. H. MacDonald, Appl. Phys. Lett. **81**, 4029 (2002).
[67]J. Wang, G. A. Khodaparast, J. Kono, T. Slupinski, A. Oiwa, and H. Munekata, Physica E **20**, 412 (2004).
[68]K. Nontapot, R. N. Kini, A. Gifford, T. R. Merritt, G. A. Khodaparast, T. Wojtowicz, X. Liu, and J. K. Furdyna, Appl. Phys. Lett. **90**, 143109 (2007).
[69]*Magneto-Optics*, edited by S. Sugano and N. Kojima (Springer-Verlag, Berlin, 2000).
[70]H. Wang, K. Ferrio, D. G. Steel, Y. Z. Hu, R. Binder, and S. W. Koch, Phys. Rev. Lett. **71**, 1261 (1993).
[71]Y. Z. Hu, R. Binder, S. W. Koch, S. T. Cundiff, H. Wang, and D. G. Steel, Phys. Rev. B **49**, 14382 (1994).
[72]K. C. Hall, G. R. Allan, H. M. van Driel, T. Krivosheeva, and W. Pötz, Phys. Rev. B **65**, 201201(R) (2002).
[73]We note that a clear band edge is typically not observed in GaMnAs due to defect-induced band tailing, which is considerable due to low-temperature growth (Ref. 20).